IL NUOVO CIMENTO Vol. 33 C, N. 5 Settembre-Ottobre 2010
DOI 10.1393/ncc/i2011-10714-4

Colloquia: LaThuile10

Recent results from BESIII

Jiaxu Zuo(*) for BESIII Collaboration
Institute of High Energy Physics, Chinese Academy of Sciences - Beijing 100049, China

(ricevuto il 14 Settembre 2010; pubblicato online l'11 Gennaio 2011)

Summary. — The BESIII experiment, running at 2–4.6 GeV center-of-mass energy, has collected the largest ψ' and J/ψ samples. New results using the data collected by the BESIII detector are presented, which include the measurement of the spin singlet state $h_c(1P)$ from ψ' decays, the χ_{c0} and χ_{c2} decays into $\pi^0\pi^0$ and $\eta\eta$ and the χ_{cJ} decays to vector meson pairs ($\omega\omega$, $\phi\phi$, $\omega\phi$). We also confirmed the $p\bar{p}$ threshold enhancement, which was observed in $J/\psi \to \gamma p\bar{p}$ at BESII, from the decays of $\psi' \to \pi^+\pi^- J/\psi(J/\psi \to \gamma p\bar{p})$ and $J/\psi \to \gamma p\bar{p}$, respectively. The X(1835) is confirmed too in $J/\psi \to \gamma\eta'\pi^+\pi^-$.

PACS 13.25.Gv – Decays of J/ψ, Υ, and other quarkonia.
PACS 14.40.Pq – Heavy quarkonia.

1. – Introduction

The upgraded Beijing Electron Positron Collider (BEPCII) is an electron-positron accelerator with separate storage rings for each beam. It is designed to run with 93 bunches for a maximum current of 910 mA per beam. The center-of-mass energy $E_{\rm CM}$ range of the e^+e^- collisions is 2.0–4.6 GeV. The designed luminosity is $1\times10^{33}\,{\rm cm}^{-2}\,{\rm s}^{-1}$ for $E_{\rm CM} = M[\psi(3770)]$ and $0.6\times10^{33}\,{\rm cm}^{-2}\,{\rm s}^{-1}$ near $M[J/\psi]$ and $E_{\rm CM} > 4\,{\rm GeV}$.

The BESIII [1] detector is designed to study the τ-charm physics [2]. The cylindrical BESIII is composed of a helium-gas based drift chamber (MDC), a Time-of-Flight (TOF) system, a CsI(Tl) Electro-Magnetic Calorimeter (EMC) and a RPC-based muon chamber (MUC) with a superconducting magnet providing 1.0 T magnetic field in the central region of BESIII. The nominal detector acceptance is 93% of 4π. The expected charged particle momentum resolution and photon energy resolution are 0.4% and 2.5% at 1 GeV, respectively. The photon energy resolution at BESIII is much better than that at BESII and comparable to those at CLEO [3] and Crystal Ball [4]. Precise measurement of energies of photons enables the BESIII experiment to study physics involving photons, π^0 and η with high accuracy. The read out system of EMC is based on FADC. To reduce incoherent noise such us beam gas and electronic noise and improve the energy resolution, a time information is recorded by counting the timing step number in FADC with a precision of 50 ns besides the read out of energy information [5].

(*) E-mail: zuojx2010@gmail.com

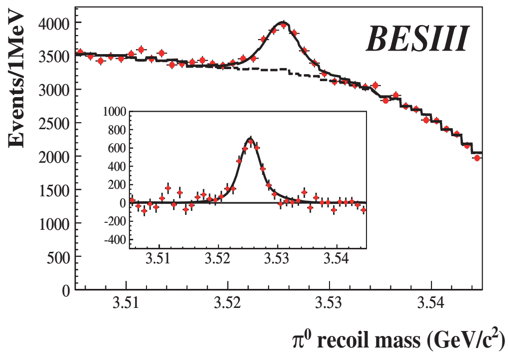

Fig. 1. – The π^0 recoil mass spectrum and fit for the $E1$-tagged analysis of $\psi' \to \pi^0 h_c, h_c \to \gamma\eta_c$. Fits are shown as solid lines, background as dashed lines. The insets show the background-subtracted spectra.

Since July 19, 2008, the first collision happened, the BESIII has collected 106M ψ' events and 226M J/ψ events which are the largest ψ' and J/ψ data samples. A continuum sample of $42.6\,\text{pb}^{-1}$ at $3.65\,\text{GeV}$ is also accumulated.

The optimization of the event selection and the estimation of physics backgrounds are performed through Monte Carlo simulations. The GEANT4-based simulation software BOOST [6] includes the geometric and material description of the BESIII detectors, the detector response and digitization models, as well as the tracking of the detector running conditions and performance. The production of the ψ' and J/ψ resonances are simulated by the Monte Carlo event generator KKMC [7], while the decays are generated by EvtGen [8] for known decay modes with branching ratios being set to the PDG [9] world average values, and by Lundcharm [10] for the remaining unknown decays. The analysis is performed in the framework of the BESIII Offline Software System (BOSS) [11] which takes care of the detector calibration, event reconstruction and data storage.

With such large data samples, the J/ψ and ψ' decay modes can be measured much more precisely than before. Using J/ψ decays, one can study light hadron spectroscopy and search for new hadronic states. With BESIII, the CKM matrix elements V_{cs}, V_{cd} and V_{us} will be extracted with an expected smaller systematic error. The $D-\bar{D}$ mixing measurement and searching for CP-violation will be possible.

2. – h_c measurement

Although the charmonium family of mesons composed of a charmed quark and its own antiquark ($c\bar{c}$) has been studied for many years, knowledge is sparse on the singlet state $h_c(^1P_1)$. Early predictions for the properties of the h_c are found in refs. [12, 13]. Many theoretical methods are used to study its branching ratios [14-16] and other physics [17]. The CLEO Collaboration first observed the h_c in the cascade process $\psi' \to \pi^0 h_c$, $h_c \to \gamma\eta_c$ in both inclusive and exclusive measurements [18-20]. The E835 experiment [21] scanned antiproton energy and observed $p\bar{p} \to h_c \to \gamma\eta_c$. We present the measurements of h_c from $\psi' \to \pi^0 h_c$, $h_c \to \gamma\eta_c$ below.

Figure 1 shows the π^0 recoil mass spectrum and fit for the $E1$-tagged analysis of $\psi' \to \pi^0 h_c$, $h_c \to \gamma\eta_c$. In E1-tagged selection, we require one photon in the energy range 465–535 MeV. The h_c signals are described by Breit-Wigner functions convoluted

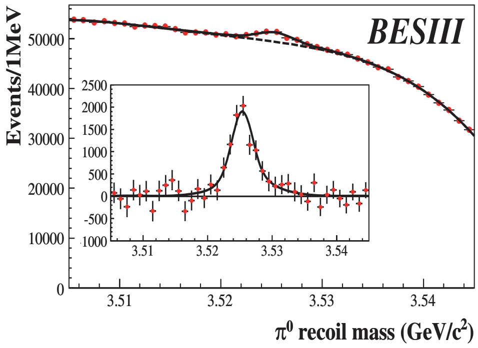

Fig. 2. – The π^0 recoil mass spectrum and fit for the inclusive analysis of $\psi' \to \pi^0 h_c$. Fits are shown as solid lines, background as dashed lines. The insets show the background-subtracted spectra.

with the instrument resolution function obtained by fitting E1-tagged h_c MC simulation. The fit results are $N^{E1} = 3679 \pm 319$, $M(h_c) = 3525.40 \pm 0.13 \pm 0.18\,\text{MeV}/c^2$, and $\Gamma(h_c) = 0.73 \pm 0.45 \pm 0.28\,\text{MeV}$ with $\chi^2/d.o.f = 33.5/36.0$ (p value 58.8%). The signal significance is $18.6\,\sigma$ for the h_c signal.

In fig. 2's fit, the mass and width of h_c are fixed to the values obtained from the E1-photon tagged analysis. The background is parameterized by a 4th-order Chebychev polynomial. The fit result is $N^{\text{tot}} = 10353 \pm 1097$ with $\chi^2/d.o.f = 24.5/34$. The signal significance is 9.5σ.

Using those fit results, we find $\mathcal{B}(\psi' \to \pi^0 h_c) = (8.4 \pm 1.3 \pm 1.0) \times 10^{-4}$, $\mathcal{B}(\psi' \to \pi^0 h_c) \times \mathcal{B}(h_c \to \gamma\eta_c) = (4.58 \pm 0.40 \pm 0.50) \times 10^{-4}$, and $\mathcal{B}(h_c \to \gamma\eta_c) = (54.3 \pm 6.7 \pm 5.2)\%$. Our measurements of $\mathcal{B}(\psi' \to \pi^0 h_c)$ and $\mathcal{B}(h_c \to \gamma\eta_c)$ and information about the h_c width are the first experimental results for these quantities. The determinations of $M(h_c)$ and $\mathcal{B}(\psi' \to \pi^0 h_c) \times \mathcal{B}(h_c \to \gamma\eta_c)$ are consistent with published CLEO results [19] and of comparable precision. The analysis results have been published [22].

3. – Confirmation of $p\bar{p}$ mass threshold enhancement and $X(1835)$

An anomalously strong $p\bar{p}$ mass threshold enhancement was observed by the BESII experiment in the radiative decay process $J/\psi \to \gamma p\bar{p}$ [23]. An interesting feature of this enhancement is that corresponding structures are not observed in near-threshold $p\bar{p}$ cross section measurements [24-28]. These non-observations disfavor the attribution of the mass-threshold enhancement to the pure effects of $p\bar{p}$ final state interactions (FSI). This observation stimulated a number of theoretical speculations [29-32]. One of these is the intriguing suggestion that it is an example of a $p\bar{p}$ bound state [33], sometimes called baryonium [34]. A resonance, the X(1835), was observed in the $\pi^+\pi^-\eta'$ invariant-mass spectrum with a statistical significance of 7.7σ at BESII [35]. The mass and width of X(1835) are not compatible with any known meson resonance. With BESIII's larger data samples, it is important to confirm those measurements. The improved measurement will be useful to understand the truth of the threshold enhancement and X(1835).

After the selection [36], we get the similar characterize of the $p\bar{p}$ mass threshold enhancement. We fit it with an acceptance weighted Breit-Wigner (BW) function of the form $BW(M) \propto \frac{q^{2L+1}k^3}{(M^2-M_0^2)^2+M_0^2\Gamma^2}$, where Γ is a constant (determined from fit), q is the

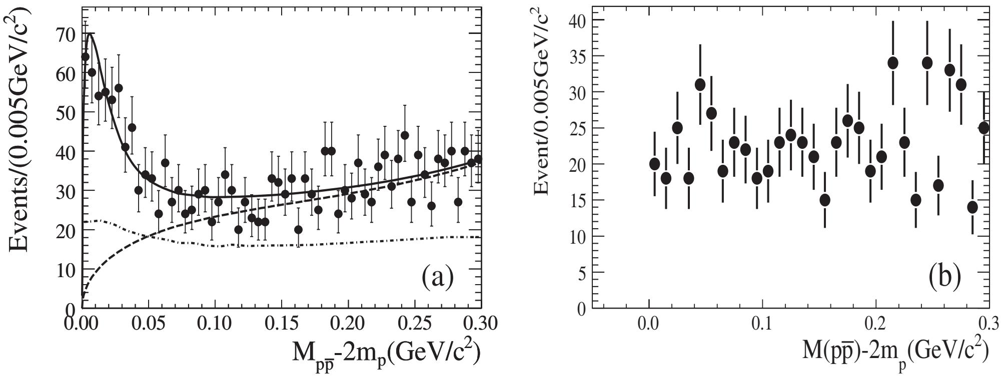

Fig. 3. – (a) The $p\bar{p}$ invariant mass spectrum for the $\psi' \to \pi^+\pi^- J/\psi(J/\psi \to \gamma p\bar{p})$ after final event selection. The solid curve is the fit result; the dashed curve shows the fitted background function, and the dash-dotted curve indicates how the acceptance varies with $p\bar{p}$ invariant mass. (b) The $p\bar{p}$ invariant mass spectrum in the threshold region for the selected $\psi' \to \gamma p\bar{p}$ candidate events with ψ' data.

proton momentum in the $p\bar{p}$ rest-frame, L is the $p\bar{p}$ orbital angular momentum, and k is the photon momentum, together with the background shape. Here, the background shape is described by the function of the form $f_{bkg}(\delta) = N(\delta^{1/2} + a_1\delta^{3/2} + a_2\delta^{5/2})$, where $\delta = M_{p\bar{p}} - 2m_p$ and the shape parameters a_1 and a_2 are determined from a fit to selected $\gamma p\bar{p}$ events for $\psi' \to \pi^+\pi^- J/\psi(J/\psi \to \gamma p\bar{p})$ phase-space MC sample. The mass spectrum fitting with S-wave ($L = 0$) in the threshold mass region of $M_{p\bar{p}} - 2m_p < 0.3\,\mathrm{GeV}/c^2$ is shown in fig. 3(a), and it yields a peak mass of $M = 1861^{+6}_{-13}\,(\mathrm{stat})^{+7}_{-26}\,(\mathrm{syst})\,\mathrm{MeV}/c^2$ and a width of $\Gamma < 38\,\mathrm{MeV}/c^2$ at the 90% CL. In the study of $\psi' \to \gamma p\bar{p}$ with ψ' data, there is no significant narrow threshold enhancement as shown in fig. 3(b). It indicates that the strong $p\bar{p}$ threshold enhancement observed in J/ψ radiative decay is disfavored for the interpretation of pure final state interactions (FSI).

For the $J/\psi \to \gamma\pi^+\pi^-\eta'(\eta' \to \gamma\rho)$ channel, the $\pi^+\pi^-\eta'$ invariant-mass spectrum for the selected events is shown in fig. 4(a) and significant peak at $M \sim 1835\,\mathrm{MeV}/c^2$ is observed. If it is fitted with one resonance plus a polynomial background shape, the statistical significance of the resonance is about 9σ as shown in fig. 4(b). In the $J/\psi \to \gamma\pi^+\pi^-\eta'(\eta' \to \pi^+\pi^-\eta, \eta \to \gamma\gamma)$ mode, the $\pi^+\pi^-\eta'$ invariant-mass spectrum for the selected events is shown in fig. 5(a) and significant peak at $M \sim 1835\,\mathrm{MeV}/c^2$ is also observed. If it is fitted with one resonance plus a polynomial background shape, the statistical significance of the resonance is about 18σ as shown in fig. 5(b).

Figure 6 shows the $\pi^+\pi^-\eta'$ invariant-mass spectrum for the combined $J/\psi \to \gamma\pi^+\pi^-\eta'(\eta' \to \gamma\rho)$ and $J/\psi \to \gamma\pi^+\pi^-\eta'(\eta' \to \pi^+\pi^-\eta)$. It is fitted with a Breit-Wigner function convolved with a Gaussian mass resolution function. The mass and width obtained from the fit are $M = 1842.4 \pm 2.8(\mathrm{stat})\,\mathrm{MeV}/c^2$ and $\Gamma = 99.2 \pm 9.2\,(\mathrm{stat})\,\mathrm{MeV}/c^2$ with a statistical significance of 21σ. These values are consistent with the published BESII results [35].

4. – χ_{cJ} to two vector meson decays

In the quark model, the χ_{cJ} ($J = 0, 1, 2$) mesons are $L = 1$ $c\bar{c}$ states. The measurements of the branching fraction of the hadronic χ_{cJ} decay channels are mandatory to

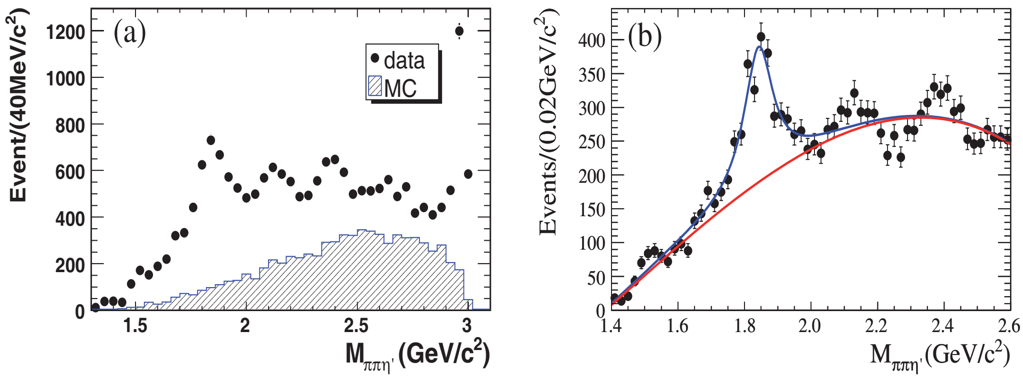

Fig. 4. – Candidate events after final event selection for $J/\psi \to \gamma\pi^+\pi^-\eta'(\eta' \to \gamma\rho)$. (a) Invariant mass spectrum of $\pi^+\pi^-\eta'$ after final selection, the solid circles are data and the shade histogram is from $J/\psi \to \gamma\pi^+\pi^-\eta'$ phase space MC events (with arbitrary normalization). (b) Mass spectrum fitting with one resonance and polynomial background shape.

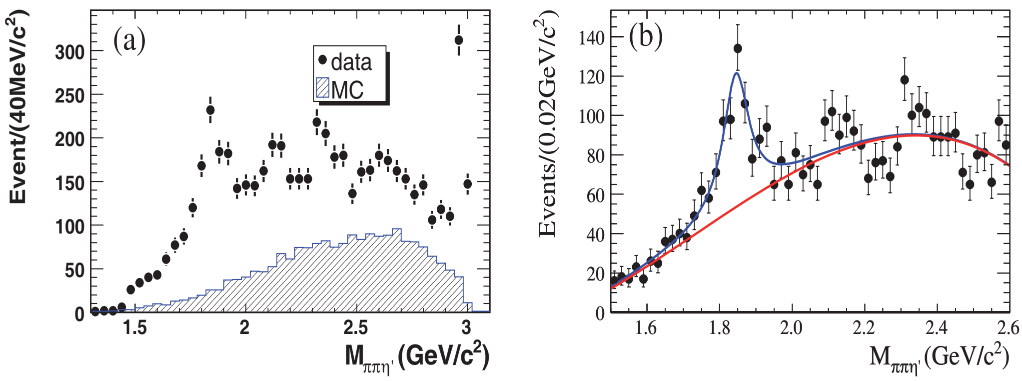

Fig. 5. – Candidate events after final event selection for $J/\psi \to \gamma\pi^+\pi^-\eta'(\eta' \to \pi^+\pi^-\eta, \eta \to \gamma\gamma)$. (a) Invariant mass spectrum of $\pi^+\pi^-\eta'$ after final selection, the solid circles are data and the shade histogram is from $J/\psi \to \gamma\pi^+\pi^-\eta'$ phase space MC events (with arbitrary normalization). (b) Mass spectrum fitting with one resonance and polynomial background shape.

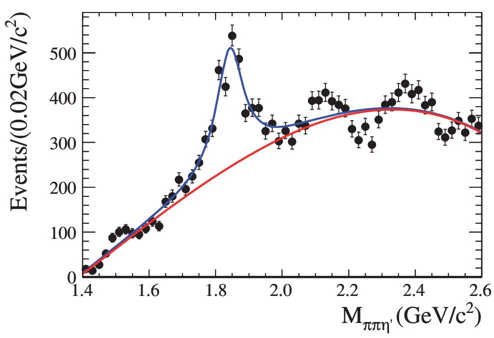

Fig. 6. – The $\pi^+\pi^-\eta'$ invariant-mass spectrum for the combined $J/\psi \to \gamma\pi^+\pi^-\eta'(\eta' \to \gamma\rho)$ and $J/\psi \to \gamma\pi^+\pi^-\eta'(\eta' \to \pi^+\pi^-\eta)$. It is fitted with a Breit-Wigner (BW) function convolved with a Gaussian mass resolution function.

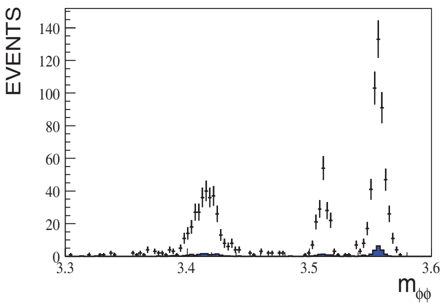

Fig. 7. – Invariant mass of $\phi\phi$ final state.

further test the Color Octet Model (COM) in P-wave charmonium decays. Some studies [37] pointed out that the decay of $\chi_{c0,2}$ into vector meson pairs (VV), pseudoscalars pairs (PP), and scalar pairs (SS) can be investigated in a general factorization scheme.

Branching fractions are only published for $\chi_{cJ} \to \phi\phi$ and $\chi_{cJ} \to \omega\omega$ according to the BESII's measurements [38] and [39]. Due to imperfect detection resolution and low statistics, we just report the observation of $\chi_{c0,2}$ at that time, hard to judge that there is any χ_{c1} signal in $\phi\phi$ and $\omega\omega$ final state. For the doubly OZI decay mode, $\chi_{cJ} \to \omega\phi$, no any measurement is available before. With the large ψ' data sample taken at BESIII, we observed the clear $\chi_{c0,1,2} \to \omega\omega, \phi\phi$. Particularly, the χ_{c1} signal is observed for the first time. Figures 7 and 8 show the $M_{\phi\phi}$ and $M_{\omega\omega}$ distribution, respectively. Clear χ_{cJ} signal can be seen. For doubly OZI decay, $\chi_{cJ} \to \omega\phi$. We also observed the clear $\chi_{c0,1}$ signal. It is shown in fig. 9.

5. – χ_{c0} and χ_{c2} decay into $\pi^0\pi^0$ and $\eta\eta$ measurement

We also study the $\chi_{c0,2}$ decay to $\pi^0\pi^0$ and $\eta\eta$ final states. Those measurement provides information on both the χ_{cJ} parents and their pseudo-scalar daughters, as well as a better understanding of the decay mechanisms of χ_{cJ} mesons [40].

The radiative photon energy spectrum of $\chi_{cJ} \to \pi^0\pi^0$ candidates, shown in fig. 10, is fitted using an unbinned maximum likelihood fit in the range from 0.06 GeV to 0.36 GeV.

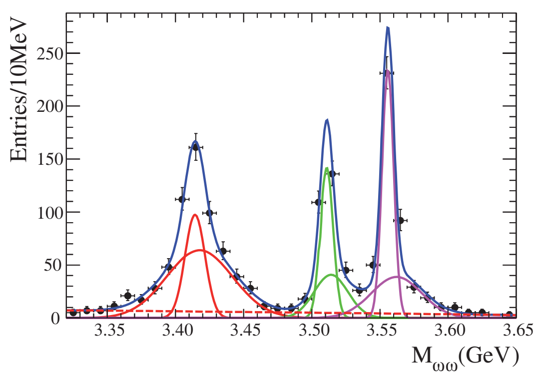

Fig. 8. – Invariant mass of $\omega\omega$ final state.

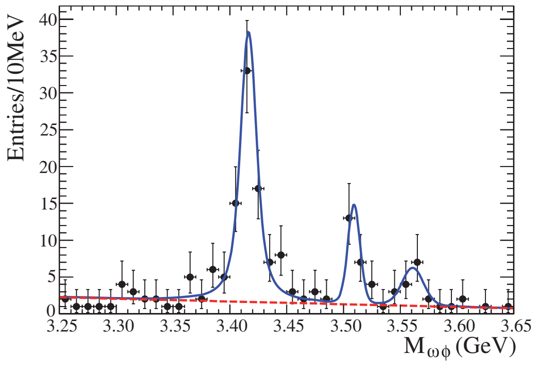

Fig. 9. – Invariant mass of $\omega\phi$ final state.

The shapes of the χ_{c0} and χ_{c2} are obtained from Monte Carlo simulation and the masses and widths of χ_{cJ} are fixed to their PDG values [9]. A 2nd-order Chebychev polynomial is used to describe the backgrounds, including those found in the inclusive MC study and the continuum. The fit gives a χ_{c0} signal yield of 17443 ± 167 events and a χ_{c2} signal yield of 4516 ± 80 events. The selection efficiency from Monte Carlo simulation of $\psi' \to \gamma\chi_{c0}(\chi_{c0} \to \pi^0\pi^0, \pi^0 \to \gamma\gamma)$ is $(55.6 \pm 0.2)\%$ and the efficiency of $\psi' \to \gamma\chi_{c2}(\chi_{c2} \to \pi^0\pi^0, \pi^0 \to \gamma\gamma)$ is $(59.8 \pm 0.2)\%$. The branching fractions are then determined to be $Br(\chi_{c0} \to \pi^0\pi^0) = (3.23 \pm 0.03 \pm 0.23 \pm 0.14) \times 10^{-3}$, $Br(\chi_{c2} \to \pi^0\pi^0) = (0.88 \pm 0.02 \pm 0.06 \pm 0.04) \times 10^{-3}$.

The fit to the radiative photon energy spectrum of $\chi_{cJ} \to \eta\eta$ candidates, shown in fig. 11, gives a χ_{c0} signal yield of 2132 ± 60 events and a χ_{c2} signal yield of 386 ± 25 events. The selection efficiency is $40.3 \pm 0.2\%$ and $43.9 \pm 0.2\%$ for $\chi_{c0} \to \eta\eta$ and $\chi_{c2} \to \eta\eta$, respectively. The branching fractions are $Br(\chi_{c0} \to \eta\eta) = (3.44 \pm 0.10 \pm 0.24 \pm 0.13) \times 10^{-3}$, $Br(\chi_{c2} \to \eta\eta) = (0.65 \pm 0.04 \pm 0.05 \pm 0.03) \times 10^{-3}$. These analysis results have been published [41].

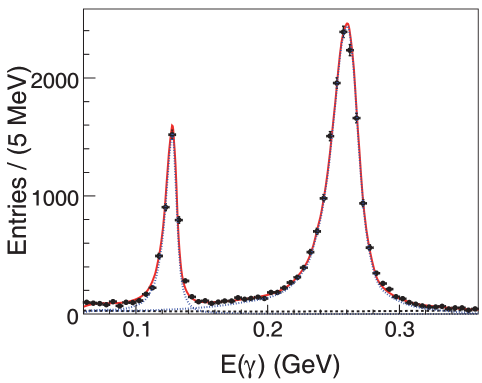

Fig. 10. – The radiative photon energy spectrum of selected $\chi_c \to \pi^0\pi^0$ events. Dots with error bars are data. The solid curve is the result of a fit described in the text. The dotted curves are the χ_{cJ} signals. The dashed curve is the background polynomial.

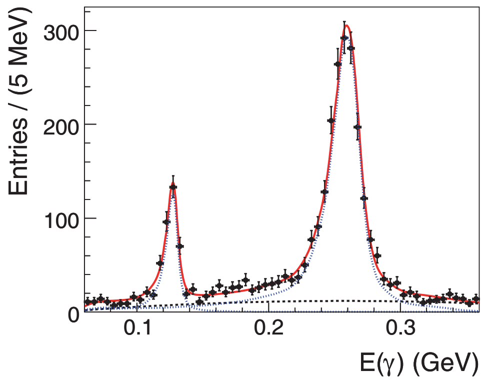

Fig. 11. – The radiative photon energy spectrum of selected $\chi_c \to \eta\eta$ events. Dots with error bars are data. The solid curve is the result of a fit described in the text. The dotted curves are the χ_{cJ} signals. The dashed curve is the background polynomial.

6. – Conclusions

With the largest sample of ψ' and J/ψ in the BESIII detector, many measurements are reported. We have performed many studies on h_c and χ_c. The $\Gamma(h_c)$, $\mathcal{B}(\psi' \to \pi^0 h_c)$ and $\mathcal{B}(h_c \to \gamma\eta_c)$ are measured for the first time. The branching fractions of $\chi_{c0,2} \to \pi^0\pi^0$ and $\chi_{c0,2} \to \eta\eta$ are measured with improved precision. We also observed the clear $\chi_{c0,1,2} \to \omega\omega, \phi\phi$. Particularly, the χ_{c1} signal and the doubly OZI decay mode, $\chi_{cJ} \to \omega\phi$, are firstly observed. The $p\bar{p}$ threshold enhancement and $X(1835)$ are studied. These results are consistent with the published BESII results.

A new facility for physics in the τ-charm region has become operational. With the running of BEPCII/BESIII, more exciting results are coming.

* * *

I would like to thank my colleagues of BESIII Collaboration. I would also like to thank the organizer for warm hospitality at La Thuile.

REFERENCES

[1] Ablikim M. *et al.* (BESIII Collaboration), *Nucl. Instrum. Methods A.*, **614** (2010) 3.
[2] Chao K. T. and Wang Y. F. (Editors), *Physics at BESIII*, *Int. J. Mod. Phys. A*, **24** (2009) No. 1 supp.
[3] Viehhausser G. *et al.*, *Nucl. Instrum. Methods A*, **462** (2001) 146.
[4] Oreglia M. *et al.*, *Phys. Rev. D*, **25** (1982) 2559.
[5] SHAN Li-Min *et al.*, *HEP & NP*, **30(11)** (2006) 1091 (in Chinese).
[6] Deng Z. Y. *et al.*, *Chin. Phys. C*, **30** (2006) 371.
[7] Jadach S., Ward B. F. L. and Was Z., *Comput. Phys. Commun.*, **130** (2000) 260; *Phys. Rev. D*, **63** (2001) 113009.
[8] Ping R. G. *et al.*, *Chin. Phys. C*, **32** (2008) 599.
[9] Amsler C. *et al.* (Particle Data Group), *Phys. Lett. B*, **667** (2008) 1.
[10] Chen J. C. *et al.*, *Phys. Rev. D*, **62** (2000) 034003.
[11] Li W.D and Liu H. M *et al.*, *The Offline Software for the BESIII Experiment, Proceedings of CHEP 2006.*

[12] Kuang Y. P., Tuan S. F. and Yan T. M., *Phys. Rev. D*, **37** (1988) 1210.
[13] Ko P., *Phys. Rev. D*, **52** (1995) 1710.
[14] Kuang Y. P., *Phys. Rev. D*, **65** (2002) 094024.
[15] Godfrey S. and Rosner J., *Phys. Rev. D*, **66** (2002) 014012.
[16] Dudek J. J., Edwards R. G. and Richards D. G., *Phys. Rev. D*, **73** (2006) 074507.
[17] See, for example, Swanson E. S., *Phys. Rep.*, **429** (2006) 243 and references therein.
[18] Rosner J. L. *et al.* (CLEO Collaboration), *Phys. Rev. Lett.*, **95** (2005) 102003; Rubin P. *et al.* (CLEO Collaboration), *Phys. Rev. D*, **72** (2005) 092004.
[19] Dobbs S. *et al.* (CLEO Collaboration), *Phys. Rev. Lett.*, **101** (2008) 182003.
[20] Adams G. S. *et al.* (CLEO Collaboration), *Phys. Rev. D*, **80** (2009) 051106.
[21] Andreotti M. *et al.* (E-835 Collaboration), *Phys. Rev. D*, **72** (2005) 032001.
[22] Ablikim M. *et al.* (BES Collaboration), *Phys. Rev. Lett.*, **104** (2010) 132002.
[23] Bai J. Z. *et al.* (BES Collaboration), *Phys. Rev. Lett.*, **91** (2003) 022001.
[24] Wang M. Z. *et al.*, *Phys. Rev. Lett.*, **92** (2004) 131801.
[25] Jin S., *Invited plenary talk at the XXXIIth International Conference on High Energy Physics(ICHEP04), Beijing, 2004*.
[26] Ablikim M. *et al.* (BES Collaboration), *Phys. Rev. Lett.*, **99** (2007) 011802.
[27] Athar S. B. *et al.* (CLEO Collaboration), *Phys. Rev. D*, **73** (2006) 032001.
[28] Ablikim M. *et al.* (BES Collaboration), *Eur. Phys. J. C*, **53** (2008) 15.
[29] Datta A. and O'Donnell P. J., *Phys. Lett. B*, **567** (2003) 273; Yan M. L. *et al.*, *Phys. Rev. D*, **72** (2005) 034027; Loiseau B. and Wycech S., *Phys. Rev. C*, **72** (2005) 011001.
[30] Ellis J., Frishman Y. and Karliner M., *Phys. Lett. B*, **566** (2003) 201; Rosner J. L., *Phys. Rev. D*, **68** (2003) 014004.
[31] Gao C. S. and Zhu S. L., *Commun. Theor. Phys.*, **42** (2004) 844, hep-ph/0308205.
[32] Ding G. J. and Yan M. L., *Phys. Rev. C*, **72** (2005) 015208.
[33] Klempt E. *et al.*, *Phys. Rep.*, **368** (2002) 119; Richard J.-M., *Nucl. Phys. Proc. Suppl.*, **86** (2001) 361.
[34] Shapiro I. S., *Phys. Rep.*, **35** (1978) 129; Dover C. B. and Goldhaber M., *Phys. Rev. D*, **15** (1977) 1997.
[35] Ablikim M. *et al.* (BES Collaboration), *Phys. Rev. Lett.*, **95** (2005) 262001.
[36] Ablikim M. *et al.* (BESIII Collaboration), *Chin. Phys. C*, **34** (2010) 4, arXiv:1001.5328.
[37] Zhao Q., *Phys. Lett. B*, **659** (2008) 221.
[38] Ablikim M. *et al.* (BES Collaboration), *Phys. Lett. B*, **642** (2006) 197.
[39] Ablikim M. *et al.* (BES Collaboration), *Phys. Lett. B*, **630** (2005) 7.
[40] Zhao Q., *Phys. Rev. D*, **72** (2005) 074001.
[41] Ablikim M. *et al.* (BES Collaboration), *Phys. Rev. D*, **81** (2010) 052005.